

Magnetoresistance anisotropy in amorphous superconducting thin films: Site-bond percolation approach

Elkana Porat and Yigal Meir*

Department of Physics, Ben-Gurion University, Beer Sheva 84105, Israel

(Received 22 October 2014; published 13 July 2015)

Recent measurements of the magnetoresistance (MR) of amorphous superconducting thin films in tilted magnetic fields have displayed several surprising experimental details, in particular, a strong dependence of the MR on the field angle at low magnetic fields, which diminishes and then changes sign at large fields. Using a generalized site-bond percolation model, which takes into account both orbital and Zeeman effects of the magnetic field, we show that the resulting MR curves reproduce the main experimental features. Such measurements, accompanied by the corresponding theory, may be crucial in pinpointing the correct theory of the superconductor-insulator transition and of the MR peak in thin disordered films.

DOI: [10.1103/PhysRevB.92.024509](https://doi.org/10.1103/PhysRevB.92.024509)

PACS number(s): 71.30.+h, 73.43.Nq, 74.20.Mn

The superconductor-insulator transition (SIT) in thin superconducting (SC) films was observed 25 years ago [1,2], yet its nature is still under debate [3], due to the interplay between superconductivity and disorder. While weak disorder has little effect on the SC state [4], strong disorder may lead to suppression of the SC state due to fluctuations of the SC order parameter [5,6]. Indeed, a SIT has been observed upon tuning of, e.g., the film thickness [1], external magnetic field [2], or disorder [7]. Over the years, several paradigms for the transition have been put forward, which can be broadly grouped into a pure bosonic paradigm, sometimes called the “dirty boson” model [8–10], and variants of the percolation model [11–17]. Further insight into the nature of the transition was made possible due to magnetoresistance (MR) measurements in the normal phase [18,19], where a giant resistance peak has been observed beyond the SIT, followed by a dramatic drop as the field is further increased. This dramatic observation has been explained by a phenomenological percolation approach [15], which emphasizes the competition between the SC and the fermionic degrees of freedom, due to the persistence of SC islands (SCIs) into the insulating phase. An alternative explanation, based on the boson-only picture, was put forward in Ref. [10], where the role of the fermionic degrees of freedom is played by vortices.

While experiments have indeed indicated the formation of SC puddles [11,20–23] and of critical (classical or quantum) percolation behavior [2,24–28], it is clear that more experimental data are needed to establish the nature of the transition and of the insulating phase. In recent years, detailed examinations of the MR dependence on the direction of the field have been performed [29,30] [see Figs. 1(a) and 1(b)]. The main observations are as follows. (i) There is highly anisotropic MR in the low-field regime, reflected by the high dependence of the MR amplitude, SIT critical field B_c , and MR peak field B_{\max} on the field direction. (ii) A lower peak resistance was measured for shallower angles. (iii) The magnitude of the anisotropy decreases with the strength of the field, up to a point beyond the peak, where the MR curves seem to converge to isotropic MR, that is, angle independent resistance at a certain magnetic field intensity B_{iso} . (iv) In

samples that are SC at zero field the anisotropy is reversed at higher fields, i.e., the resistance is higher for shallower angles [29], while samples that are insulating at zero field depict nearly isotropic behavior for all $B > B_{\text{iso}}$ [30].

These new results are yet to be accounted for in any of the theoretical pictures for the SIT and, thus, are a key observation to discern the correct theory. In this paper we demonstrate that a phenomenological model within the framework of the percolation model can explain these observations (see Fig. 1). This gives further credibility to the percolation description of the SIT and sheds light on the different effects of the magnetic field.

The percolation theory of the MR of disordered SC thin films in a perpendicular field is based on three assumptions [15]. (i) The disorder induces fluctuations of the order parameter, which, beyond the SIT, results in the formation of SCIs with nonzero pairing amplitude. This is supported by numerical [12,17] and experimental [11,20–23] data. (ii) Some of these SCIs are coherently coupled, forming a larger SC cluster. The concentration and size of these SC clusters are monotonically reduced under an external magnetic field, presumably due to vortex penetration, which destroys the coherence between SCIs that form a single SC cluster. This results in a separation of the SC cluster into several smaller clusters. This picture is supported in numerical calculations [16], taking into account phase correlations. (iii) Tunneling of electrons to SCIs is suppressed due to a charging energy or weak Andreev tunneling.

Under these assumptions, the SIT was interpreted [15] as a percolation transition, where the coherent SC clusters cease to span the sample as their concentration is reduced below the percolation threshold. The MR peak was described as a crossover between Cooper-pair transport through the SCIs, via incoherent Josephson couplings [31], and electron current, avoiding the SCIs because of the suppressed tunneling. However, this theory, based on orbital effects of the magnetic field, cannot capture all of the recent observations. For example, if only orbital effects mattered, the MR curves at different angles would collapse onto each other upon appropriate scaling of the magnetic field, in contrast with observations (ii)–(iv). Here we include two independent mechanisms, orbital and Zeeman effects, whose relative importance, as shown below, varies with field amplitude and angle. The interplay of these two

*ymeir@bgu.ac.il

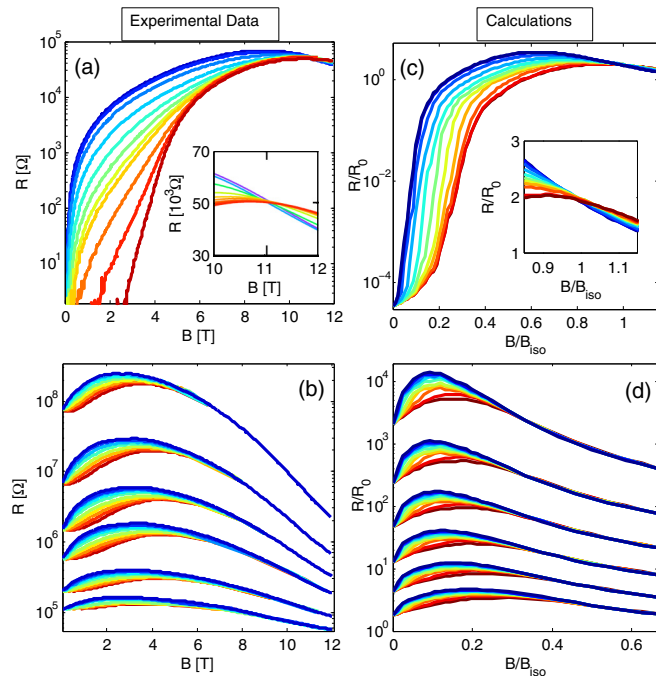


FIG. 1. (Color online) (a) MR isotherms from Ref. [29], for a sample which is a superconductor at zero field. The traces differ in the angle θ of the magnetic field B , with respect to the plane of the sample, from $\theta = 0^\circ$, plotted in dark red, to 90° , plotted in dark blue. Inset: The resistance is isotropic at the crossing point at $B_{\text{iso}} = 11.02T$. (b) MR isotherms from Ref. [30], for a sample which is insulating at zero field. Temperatures range between $T = 1$ K and $T = 0.3$ K (bottom group to top group). In each group of curves, colors represent different angles of B , from $\theta = 0^\circ$ (dark red) to 90° (dark blue). (c) Site-bond percolation results for low disorder (small Δ_0 ; see text); the sample is initially in the SC phase. Data were log-averaged [$\log(R) = \frac{1}{N} \sum_i \log(R_i)$] over $N = 100$ disorder realizations of a sample with 25×25 sites, at tilt angles similar to that in Fig. 1(a), with the parameters $\Delta_0 = 0.25$, $x = 300$, $n = 0.5$, $W = 0.4$, $E_c = 4$, $T = 1$, and $\chi = 0.05$. The magnetic field is normalized by the isotropic field $B_{\text{iso}} = 0.6$. (d) Site-bond percolation results for high disorder (larger Δ_0); the sample is in the insulating phase. Data were log-averaged over 200 realizations of a sample with 25×25 sites, at tilt angles similar to that in Fig. 1(b), with the model parameters $\Delta_0 = 0.6$, $x = 1000$, $n = 0.5$, $W = 0.4$, $E_c = 4$, and $\chi = 0.01$ and temperatures $T = 0.05, 0.07, 0.1, 0.15, 0.25$, and 0.5 (top to bottom).

field effects has already been investigated numerically [16,17], and the effect of the Zeeman field may be summarized by the following two conclusions: (a) An increase in this field results in consecutive and separate collapses of SCIs, due to the competition between the energy scales of the SC gap and the Zeeman energy [32,33]; and (b) an increase in the orbital field decreases the average SC order parameter, thus allowing SCI collapse at a smaller Zeeman field. It is the latter point, the fact that the impact of the Zeeman field depends also on the orbital field, which will lead to the reversed anisotropy at a sufficiently high field.

The underlying physics is as follows. The disorder determines the concentration of the SCIs in the sample at zero field. These SCIs may be coherently coupled to form a large

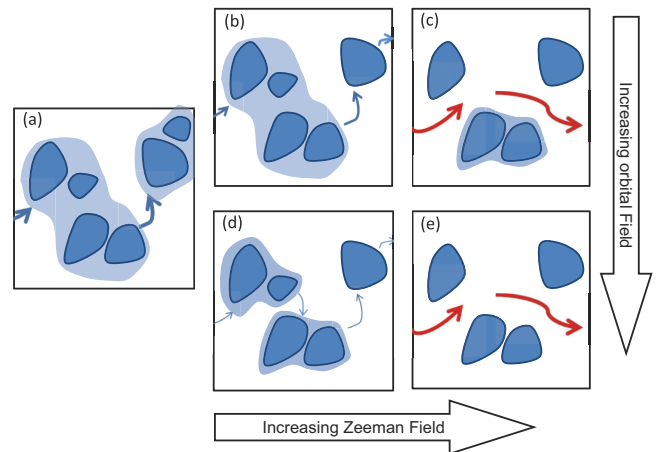


FIG. 2. (Color online) Schematic of the combined effects of the Zeeman and orbital magnetic fields. (a) At a relatively low magnetic field, adjacent SCIs (dark-blue shapes) maintain phase coherence, thus forming larger SC clusters (light-blue aura). Most of the current is carried by SC paths, i.e., paths which include SCIs (thick blue arrows). (b) As a Zeeman field is added, some of the smaller islands collapse and the total resistance increases. (c) At a sufficiently high Zeeman field the SC paths become unfavorable compared to the purely normal paths (red arrows), and normal current becomes dominant. From this point on isotropic or negative MR is observed. (d) When orbital (perpendicular) field is added to the Zeeman field of frame (b), some of the intercorrelations between adjacent SCIs are destroyed due to vortex penetration. This results in an increased total resistance, compared to a parallel field of the same amplitude. (e) When normal paths are dominant, the intercoherence of adjacent SCIs, determined by the orbital field, becomes unimportant, and the resistance becomes isotropic with respect to the direction of the field.

SC cluster, if the Josephson coupling is large enough to overcome quantum and temperature fluctuations. If an SC cluster percolates through the system, it is a superconductor, but with increasing orbital field, vortices penetrate the system, weakening the Josephson coupling between the SCIs and, eventually, leading to loss of percolation, manifested by the SIT. This effect is highly anisotropic, due to the two-dimensionality of the system. SC order can also be lost by the isotropic Zeeman effect, which leads to the collapse of individual SCIs, when it exceeds the local SC gap. At large fields, where SCIs are few and small, the charge transport avoids SCIs due to the tunneling cost. At that point the coherence among the SCIs, determined by the orbital field, becomes irrelevant, and thus only the isotropic Zeeman field, affecting the overall area of the SCIs, changes the resistance. This leads to the isotropic behavior seen at large fields. A further increase in the orbital field would lower the typical SC gap, thus facilitating collapse of SCIs, which results in decreased resistance and, consequently, in reversed anisotropy. This physics is schematically demonstrated in Fig. 2, where we show how an orbital field affects the resistance at low fields [Figs. 2(b) and 2(d)], while having no effect at large fields [Figs. 2(c) and 2(e)].

To describe this physics quantitatively we introduce a site-bond percolation model, where the sites describe the SCIs and the links the coherence between them. We associate a uniform

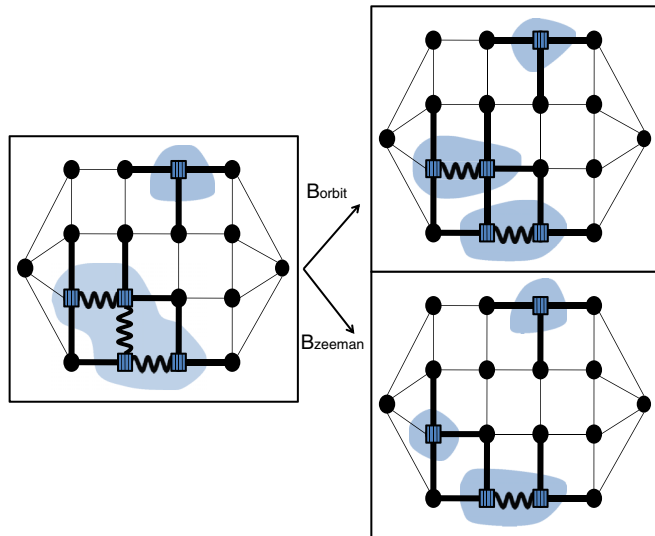


FIG. 3. (Color online) Site-bond lattice model. Left panel: The lattice sites represent either SCIs (squares) or normal regions (small circles). The concentration of SC sites is determined by disorder. Phase coherent SC sites are connected by SC bonds (wavy lines), thus forming large SC clusters [shaded (blue) areas]. A large blockade resistance (thick line) connects normal and SC sites. As orbital field is added (top-right panel), coherence between adjacent sites is suppressed, and some of the SC bonds are broken and replaced with blockade bonds. As a result, SC clusters may decompose into smaller clusters. Addition of Zeeman field (bottom-right panel) results in the collapse of some of the SC sites into normal sites, which results in an increase in normal paths (thin lines).

distribution of local gaps $P(\Delta_i)$ with the sites, such that any site with $\Delta_i > \Delta_0$ is considered SC (small squares in Fig. 3). Thus Δ_0 describes the amount of disorder in the system. The Zeeman field B causes further destruction of SC sites, for which $\Delta_i - \Delta_0 < B$. At zero field all nearest-neighbor SCIs are connected coherently, forming a larger SC cluster (shaded areas in Fig. 3). The orbital field $B_{\perp} \equiv B \sin \theta$, where θ is the angle between the field and the plane, has two effects: (a) Due to the penetration of vortices, the concentration of SC links $p_b(B_{\perp})$ decreases, causing the possible breakdown of a larger SC cluster into smaller ones; and (b) the orbital field affects $P(\Delta_i)$, the distribution of the local SC gap. An illustration of these effects of the orbital and Zeeman fields is presented in Fig. 3. Quantitatively, to account for (a), we choose, at small fields, $p_b(B_{\perp}) = 1 - x \cdot B_{\perp}^2$, assuming a symmetric and analytic response to the field. At higher fields, however, the dynamics of the vortex penetration changes. While the number of vortices is proportional to the field, they tend to congregate in specific places where the energy gap is small. Thus the number of vortices that destroy SC links is effectively smaller. We model this behavior by replacing the orbital response function at large fields with $p_b(B_{\perp}) = 1 - B_{\perp}^n$, $n < 1$. The crossover between the regions of small and large fields is arbitrarily chosen as $x B_{\perp}^2 = B_{\perp}^n$. The second effect of the orbital field is described in Ref. [17] as a shift of the gap distribution towards 0. This is manifested in the model by a uniform shift of all the local gaps by the vortex concentration, $\Delta_i \rightarrow \Delta_i - \chi \cdot p_b(B_{\perp})$, where χ is the coupling factor.

In order to calculate the resistance of the sample, we assign resistances to the links. The resistance between nearest-neighbor normal sites is activated [34], $R_{ij} = R_0 \exp^{(|\epsilon_i| + |\epsilon_j| + |\epsilon_i - \epsilon_j|) / k_B T}$, where ϵ_i is the energy of site i , and T is the temperature. The site energies are taken from a uniform distribution $[-W/2, W/2]$, where W determines the disorder in energy. On the other hand, the resistance of the SC links $R_{SC}(T)$ is taken to be very small compared to R_0 and vanishes as $T \rightarrow 0$. The precise functional form of $R_{SC}(T)$ has no qualitative influence on the results and was arbitrarily taken to be a power law, $R_{SC} \sim T^{1/2}$. The resistance between SC and normal sites or between near-neighbor uncorrelated SC sites represents the charging energy required for electrons to enter the SCIs, thus their resistance is given by

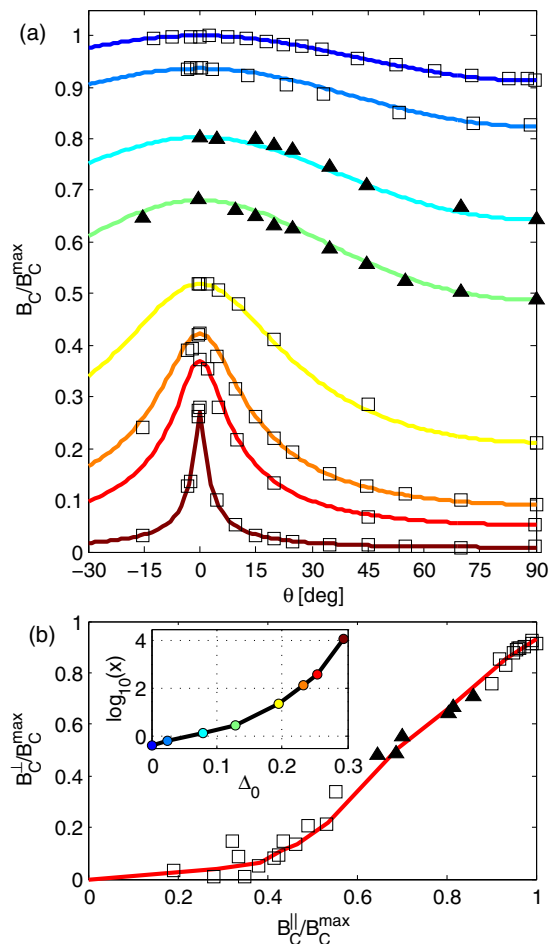


FIG. 4. (Color online) (a) Measured SIT critical field (open squares) and peak field (filled triangles) of several films, for different orientations of B with respect to the plane of the film, taken from Ref. [29]. Solid lines correspond to solutions of Eq. (1), under the assumption of a square two-dimensional lattice and fitted Δ_0 and x . Fitted parameters are presented in the inset in (b). Both experimental and theoretical data are scaled by the largest critical field, representing the case of a clean system and parallel field. (b) Measured perpendicular versus parallel critical magnetic fields and peak fields (open squares and filled triangles, respectively), taken according to Ref. [29], together with fitted model data (solid line). Inset: The fitted parameters, presented as $\log_{10}(x)$, versus the corresponding Δ_0 . Circles represent the data in (a), with corresponding colors.

$R_B = R_{B0} \exp[\tilde{E}_{c,i}/(k_B T)]$, where $\tilde{E}_{c,i}$ is the charging energy of the site, and we used $R_{B0} = R_0$ throughout the calculations. $\tilde{E}_{c,i}$ was chosen to be inversely proportional to the island size $\tilde{E}_{c,i} \sim E_c/S_i$, where the cluster size S_i is defined by the number of sites connected to site i by SC bonds (the MR was not qualitatively sensitive to the different choices for the relation of \tilde{E}_c and S).

Two representative results are displayed in Figs. 1(c) and 1(d). The main features of the experimental data [Figs. 1(a) and 1(b)] are clearly reproduced, including the strong anisotropy at low fields, which becomes weaker and then inverted at high fields, in accordance with the physics described above. The features are quite general, weakly dependent on model parameters, though the existence of a single crossing point B_{iso} in Fig. 1(c) is only achieved for specific parameter choices.

The experiment also determined the dependence of the critical magnetic field B_c on the tilt angle. In order to make comparisons with these experimental observations, one does not need to employ the full resistor network calculation, but, in fact, we can utilize an approximate formula for the site-bond percolation critical curve [35],

$$\frac{\log p_s}{\log P_C^s} + \frac{\log p_b}{\log P_C^b} = 1, \quad (1)$$

where p_s and p_b are the critical site and bond concentrations for the site-bond percolation problem, and $P_C^{s(b)}$ are the pure site (bond) percolation thresholds. Substituting the dependence of the site and bond concentrations on the magnetic field gives a transcendental equation for B_c : $1 - \Delta_0 - B_c = P_C^s \cdot (1 - x(B_c \sin \theta)^2)^{-\alpha}$, where $\alpha \equiv \log P_C^s / \log P_C^b$. The latter equation can be solved numerically for the orientation dependence of the SIT critical magnetic field. In Fig. 4(a), the angular dependence of the critical field as measured in Ref. [29] is plotted against best-fit solutions of Eq. (1), using the critical

thresholds of a square two-dimensional lattice. As shown, a very good agreement can be achieved by fitting only two parameters. In Fig. 4(b) the measured anisotropy is presented in terms of perpendicular versus parallel critical fields, together with the fitted model prediction.

To conclude, we have addressed in this paper the MR in thin SC disordered films as a function of the field direction. The experimental data provide both qualitative and quantitative constraints on possible theories and may be crucial in pointing towards the correct theory that describes the SIT and the huge MR peak in the normal phase. In order to be able to explain the experimental features, in particular, the diminishing anisotropy with increasing field amplitude, one has to invoke both the orbital effect of the field and the Zeeman effect. Moreover, the interplay between the two is crucial to explain the high-field behavior: the orbital field facilitates collapse of the SCIs by the Zeeman field, which, at high fields, suppresses the resistance. Rather unexpectedly, the MR angle dependence suggests that the Zeeman effect has a non-negligible effect also at perpendicular fields of relatively small magnitude, particularly beyond the SIT. The comparison between the experimental data and the numerical results raises a couple of interesting questions. First, the zero-field insulating sample exhibits small negative MR at a small parallel field, which is currently not explained by our model. Second, while the observation of a single isotropic point can be explained by the numerical calculations for a limited set of parameters, it is not clear whether this is a coincidence or there are generic relations between the parameters of the model. Since such a crossing point has been reported in a single sample, we hope that this study will stimulate additional such experiments, in order to pinpoint the physics underlying the SIT and the MR peak.

We acknowledge discussions with M. Schechter and support from the Israel Science Foundation (ISF).

-
- [1] D. B. Haviland, Y. Liu, and A. M. Goldman, Onset of superconductivity in the two-dimensional limit, *Phys. Rev. Lett.* **62**, 2180 (1989).
 - [2] A. F. Hebard and M. A. Paalanen, Magnetic-field-tuned superconductor-insulator transition in two-dimensional films, *Phys. Rev. Lett.* **65**, 927 (1990).
 - [3] A. M. Goldman, Superconductor-insulator transitions of quench-condensed films, *Low Temp. Phys.* **36**, 884 (2010).
 - [4] P. W. Anderson, Theory of dirty superconductors, *J. Phys. Chem. Solids* **11**, 26 (1959).
 - [5] A. Kapitulnik and G. Kotliar, Anderson localization and the theory of dirty superconductors, *Phys. Rev. Lett.* **54**, 473 (1985).
 - [6] M. Ma and P. A. Lee, Localized superconductors, *Phys. Rev. B* **32**, 5658 (1985).
 - [7] D. Shahar and Z. Ovadyahu, Superconductivity near the mobility edge, *Phys. Rev. B* **46**, 10917 (1992).
 - [8] M. P. A. Fisher, G. Grinstein, and S. M. Girvin, Presence of quantum diffusion in two dimensions: Universal resistance at the superconductor-insulator transition, *Phys. Rev. Lett.* **64**, 587 (1990).
 - [9] M. P. A. Fisher, Quantum phase transitions in disordered two-dimensional superconductors, *Phys. Rev. Lett.* **65**, 923 (1990).
 - [10] V. M. Galitski, G. Refael, M. P. A. Fisher, and T. Senthil, Vortices and quasiparticles near the superconductor-insulator transition in thin films, *Phys. Rev. Lett.* **95**, 077002 (2005).
 - [11] D. Kowal and Z. Ovadyahu, Disorder induced granularity in an amorphous superconductor, *Solid State Commun.* **90**, 783 (1994).
 - [12] A. Ghosal, M. Randeria, and N. Trivedi, Role of spatial amplitude fluctuations in highly disordered *s*-wave superconductors, *Phys. Rev. Lett.* **81**, 3940 (1998).
 - [13] E. Shimshoni, A. Auerbach, and A. Kapitulnik, Transport through quantum melts, *Phys. Rev. Lett.* **80**, 3352 (1998).
 - [14] N. Mason and A. Kapitulnik, Dissipation effects on the superconductor-insulator transition in 2D superconductors, *Phys. Rev. Lett.* **82**, 5341 (1999).
 - [15] Y. Dubi, Y. Meir, and Y. Avishai, Theory of the magnetoresistance of disordered superconducting films, *Phys. Rev. B* **73**, 054509 (2006).

- [16] Y. Dubi, Y. Meir, and Y. Avishai, Nature of the superconductor-insulator transition in disordered superconductors, *Nature* **449**, 876 (2007).
- [17] Y. Dubi, Y. Meir, and Y. Avishai, Island formation in disordered superconducting thin films at finite magnetic fields, *Phys. Rev. B* **78**, 024502 (2008).
- [18] V. F. Gantmakher, M. V. Golubkov, J. G. S. Lok, and A. K. Geim, Giant negative magnetoresistance of semi-insulating amorphous indium oxide films in strong magnetic fields, *J. Exp. Theor. Phys.* **82**, 951 (1996).
- [19] G. Sambandamurthy, L. W. Engel, A. Johansson, and D. Shahar, Superconductivity-related insulating behavior, *Phys. Rev. Lett.* **92**, 107005 (2004).
- [20] N. Mason and A. Kapitulnik, True superconductivity in a two-dimensional superconducting-insulating system, *Phys. Rev. B* **64**, 060504 (2001).
- [21] D. Kowal and Z. Ovadyahu, Scale dependent superconductor-insulator transition, *Physica C: Supercond.* **468**, 322 (2008).
- [22] B. Sacépé, C. Chapelier, T. I. Baturina, V. M. Vinokur, M. R. Baklanov, and M. Sanquer, Disorder-induced inhomogeneities of the superconducting state close to the superconductor-insulator transition, *Phys. Rev. Lett.* **101**, 157006 (2008).
- [23] A. Kamlapure, T. Das, S. C. Ganguli, J. B. Parmar, S. Bhattacharyya, and P. Raychaudhuri, Emergence of nanoscale inhomogeneity in the superconducting state of a homogeneously disordered conventional superconductor, *Sci. Rep.* **3**, 2979 (2013).
- [24] A. Yazdani and A. Kapitulnik, Superconducting-insulating transition in two-dimensional *a*-MoGe thin films, *Phys. Rev. Lett.* **74**, 3037 (1995).
- [25] N. Marković, C. Christiansen, and A. M. Goldman, Thickness-magnetic field phase diagram at the superconductor-insulator transition in 2D, *Phys. Rev. Lett.* **81**, 5217 (1998).
- [26] M. A. Steiner, N. P. Breznay, and A. Kapitulnik, Approach to a superconductor-to-Bose-insulator transition in disordered films, *Phys. Rev. B* **77**, 212501 (2008).
- [27] R. Schneider, A. G. Zaitsev, D. Fuchs, and H. v. Löhneysen, Superconductor-insulator quantum phase transition in disordered FeSe thin films, *Phys. Rev. Lett.* **108**, 257003 (2012).
- [28] M. M. Mehta, D. A. Dikin, C. W. Bark, S. Ryu, C. M. Folkman, C. B. Eom, and V. Chandrasekhar, Magnetic field tuned superconductor-to-insulator transition at the LaAlO₃/SrTiO₃ interface, *Phys. Rev. B* **90**, 100506 (2014).
- [29] A. Johansson, I. Shammass, N. Stander, E. Peled, G. Sambandamurthy, and D. Shahar, Angular dependence of the magnetic-field driven superconductor-insulator transition in thin films of amorphous indium-oxide, *Solid State Commun.* **151**, 743 (2011).
- [30] I. Shammass, O. Cohen, M. Ovadia, I. Gutman, and D. Shahar, Superconducting correlations in thin films of amorphous indium oxide on the insulating side of the disorder-tuned superconductor-insulator transition, *Phys. Rev. B* **85**, 140507 (2012).
- [31] V. M. Galitski and A. I. Larkin, Disorder and quantum fluctuations in superconducting films in strong magnetic fields, *Phys. Rev. Lett.* **87**, 087001 (2001).
- [32] A. M. Clogston, Upper limit for the critical field in hard superconductors, *Phys. Rev. Lett.* **9**, 266 (1962).
- [33] B. S. Chandrasekhar, A note on the maximum critical field of high-field superconductors, *Appl. Phys. Lett.* **1**, 7 (1962).
- [34] A. Miller and E. Abrahams, Impurity conduction at low concentrations, *Phys. Rev.* **120**, 745 (1960).
- [35] M. Yanuka and R. Englman, Bond-site percolation: Empirical representation of critical probabilities, *J. Phys. A: Math. Gen.* **23**, L339 (1990).